



Bayesian epidemiological modeling over high-resolution network data

Stefan Engblom^{a,*}, Robin Eriksson^a, Stefan Widgren^b

^a Division of Scientific Computing, Department of Information Technology, Uppsala University, SE-751 05 Uppsala, Sweden

^b Department of Disease Control and Epidemiology, National Veterinary Institute, SE-751 89 Uppsala, Sweden

ARTICLE INFO

Keywords:

Bayesian parameter estimation
Pathogen detection
Disease intervention
Synthetic likelihood
Spatial stochastic models

ABSTRACT

Mathematical epidemiological models have a broad use, including both qualitative and quantitative applications. With the increasing availability of data, large-scale *quantitative* disease spread models can nowadays be formulated. Such models have a great potential, e.g., in risk assessments in public health. Their main challenge is model parameterization given surveillance data, a problem which often limits their practical usage. We offer a solution to this problem by developing a Bayesian methodology suitable to epidemiological models driven by network data. The greatest difficulty in obtaining a concentrated parameter posterior is the quality of surveillance data; disease measurements are often scarce and carry little information about the parameters. The often overlooked problem of the model's identifiability therefore needs to be addressed, and we do so using a hierarchy of increasingly realistic known truth experiments. Our proposed Bayesian approach performs convincingly across all our synthetic tests. From pathogen measurements of shiga toxin-producing *Escherichia coli* O157 in Swedish cattle, we are able to produce an accurate statistical model of first-principles confronted with data. Within this model we explore the potential of a Bayesian public health framework by assessing the efficiency of disease detection and -intervention scenarios.

1. Introduction

Mathematical and computational modeling are the dominating approaches in the analysis of the dynamics of diseases. The latter approach becomes increasingly important as the amount of relevant data grows. Large-scale computational epidemiological models have been successfully employed to evaluate and inform disease mitigation strategies (Ferguson et al., 2003, 2005; Germann et al., 2006; Degli Atti et al., 2008; Merler et al., 2015; Brooks-Pollock et al., 2014b). With the increasing qualities of data, the possibility of enhancing the resolution through data integration down to the scale of single individuals in a large population has also been realized (Eubank et al., 2004; Ferguson et al., 2005; Balcan et al., 2009; Merler et al., 2011; Brooks-Pollock et al., 2014b). In similar spirit, detailed contact data has been used to drive models of disease spread at various population sizes (Salathé et al., 2010; Stehlé et al., 2011; Bajardi et al., 2012; Obadia et al., 2015; Toth et al., 2015; Brooks-Pollock et al., 2014b). Data-driven models have aided in an understanding of epidemic outbreaks and endemic conditions on scales and at a level of detail that were not previously possible (Ferguson et al., 2005; Bajardi et al., 2012; Zhang et al., 2017; Liu et al., 2018; Widgren et al., 2018; Brooks-Pollock et al., 2014b).

Many infectious human diseases have a zoonotic origin, e.g., salmonellosis or infection by shiga toxin-producing *Escherichia coli* O157

(STEC O157) (European Food safety authority and European Centre for Disease Prevention and Control, 2012, 2014). Taking a *One Health* perspective, we argue that to address challenges with existing and emerging threats of zoonotic disease, the aim for computational animal disease models should be to take their place as an integrated part in public health evaluations. This clearly puts high demands on the accuracy and the way any modeling uncertainties are handled. Indeed, an outstanding difficulty with most disease spread models is parameterization, an issue often solved via mosaic approaches (Ferguson et al., 2005; Merler et al., 2011; Widgren et al., 2018; Fournié et al., 2018; Brouwer et al., 2018), that is, relying on a combination of published parameters and residual minimization schemes conditioned on the data at hand. This typically leads to parameter point estimates which always leave some doubts on the model's explanatory power. In this respect Bayesian modeling approaches (McKinley et al., 2018; Brooks-Pollock et al., 2014b) are clearly favored through their ability to consistently address probabilistic hypotheses.

The main contribution of this paper is a feasibility demonstration of Bayesian parameterization in a first-principle and data-driven national scale epidemiological model. Moreover, this is achieved under realistic assumptions as to the available pathogen measurements. Specifically, we do not require detailed sampling of large parts of the underlying epidemiological state, but only rely on detection protocols at the single-

* Corresponding author.

E-mail addresses: stefane@it.uu.se (S. Engblom), robin.eriksson@it.uu.se (R. Eriksson), stefan.widgren@sva.se (S. Widgren).

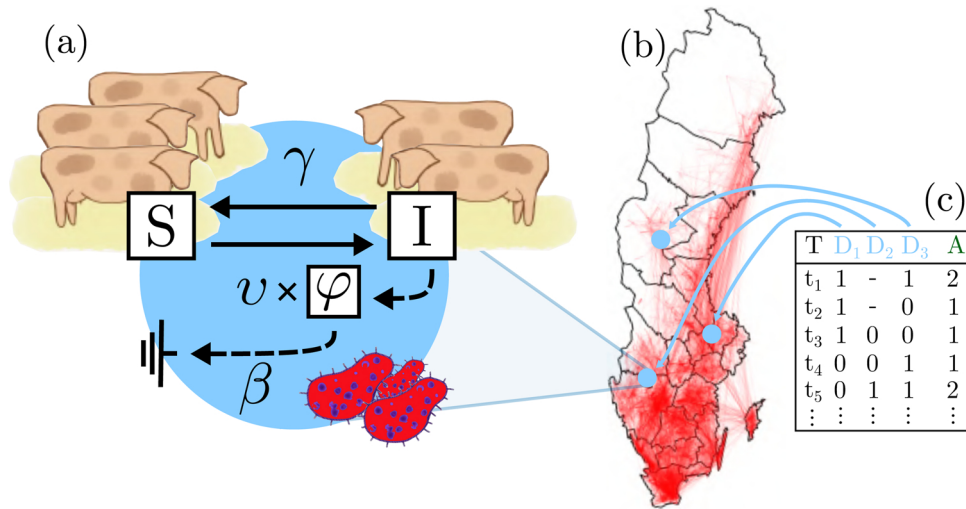


Fig. 2.1. (a) The SIS_E three parameter model. Susceptible individuals S turn infected at rate $v \times \varphi$. Infected individuals I recover at a rate γ , and shed the pathogen to the environment adding to the infectious pressure φ , which decays at rate β . (b) National transport data form the dynamic contact network in the simulations (Sweden). (c) Time series data D_1 – D_3 from single node measurements (0: not detected pathogen, 1: detected pathogen, -: missing measurement). This data is summed up and the aggregated series A is passed to the Bayesian inference procedure.

node level. For this purpose we consider a general class of disease spread models governed by two transmission processes: within-node spread coupled with a between-node spread via a transportation network. Technically, the Bayesian posterior exploration algorithm we develop is based on bootstrapped synthetic likelihoods and an adaptive Markov-chain Monte Carlo algorithm.

An often overlooked issue is the model's *identifiability*. That is, the fundamental possibility of accurately deducing the model's parameters, either in the limit of increasing amounts of data, or more practically, for the data that is actually available. We analyze this experimentally through a hierarchy of increasingly realistic data-synthetic experiments. In this way we monitor the successive complications due to increasingly realistic observational data. Arguably, in many applications the most challenging issue is the sparsity of disease measurement data. The actual information content of even relatively expensive measurements is shallow and tells little about the model's dynamics. Despite this challenge, we are able to demonstrate the feasibility of Bayesian parameterization using actual measurements taken from a study of the spread of STEC O157 in cattle (Widgren et al., 2015), and this data is sparse, noisy, and (seemingly at least) weakly informative.

With our holistic Bayesian modeling approach, a clear improvement of the public health's arsenal of tools related to zoonotic diseases is possible. To highlight this the paper is concluded by putting this idea to the test in realistic detection- and intervention scenarios.

2. Methods

Our methodology is fully simulation-based and consists of a stochastic epidemiological model and an associated simulation engine confronted with measurements via Bayesian methods driven by synthetic likelihoods (Wood, 2010). To initially judge the model's identifiability we first approach the parameterization using simpler approximate Bayesian methods and synthetic data with an available ground-truth. Upon success, full posterior exploration via synthetic likelihoods and adaptive Metropolis sampling is attempted, yielding an overall useful parameterized model. To critically assess the quality of the inference procedure we employ a version of *parametric bootstrap*, and the Bayesian model itself may of course be validated against external sources whenever possible.

Below, we first summarize the epidemiological model and the data driving the simulations in Sections 2.1 and 2.2. The Bayesian methodology is worked through in detail in Section 2.3–2.5.

2.1. The epidemiological model

In our computations we used the *SimInf* epidemiological engine (Widgren et al., 2019), which allows completely general disease spread models to be formulated. However, with the specifics of the STEC O157 application in mind, the model we have come to favor is the SIS_E model (Anderson and May, 1981, Chap. 11), which contains three state variables, $[S, I, \varphi]$, and which is defined firstly by the Markovian transitions between the integer (counting) compartments,

$$S \xrightarrow{v\varphi} I, \quad I \xrightarrow{\gamma} S, \tag{2.1}$$

that is, susceptible individuals turn infected at a rate proportional to the concentration of infectious matter φ , and infected individuals recover at rate γ . Secondly, the environmental variable φ represents the local environmental pathogen load and obeys the non-dimensionalized deterministic dynamics (Engblom and Widgren, 2017)

$$\varphi'(t) = I(S + I)^{-1} - \beta\varphi, \tag{2.2}$$

in which infected individuals shed infectious matter into the environment, which decays at a fixed rate β . While the basic SIS_E model can certainly be extended in various ways, we have found that, in practice, (2.1) and (2.2) balance model complexity with typically available data quite well. The SIS_E model is schematically summarized in Fig. 2.1 (a).

Using *SimInf*, we connect local copies of the SIS_E model with transports of individuals over a dynamic network, thus forming our population of interest. These movements are either synthetically generated or are pre-recorded movements from an actual transport network, cf. Fig. 2.1(b).

In summary, our epidemiological model consists of a three-parameter local SIS_E model in the form of a continuous-time Markov chain for (S, I) , and an ordinary differential equation for φ , connected over a network of nodes using recorded transport data at the level of batches of animals. For the specific STEC O157 application, in order to better fit data collected from a country with fairly large climate variations (Sweden), the decay parameter β was separated into seasons ($\beta_{1,2,3,4}$) for [spring, summer, fall, winter], with the simplifying assumption that spring and fall are equivalent ($\beta_1 = \beta_3$). Temperature data from the Swedish Meteorological and Hydrological Institute was used to locally determine the duration of the seasons.

2.2. Data-driven simulations and pathogen data

While there are several options to emulate network contact details, we have utilized explicit data from the Swedish national cattle database (Nöremark et al., 2011; Widgren et al., 2016). The database contains information about the individual animals in the population, including birth/death dates and movement records. The data were transformed into anonymized events for eight years of simulation over 37,220 nodes, and consist of 5,470,039 events, of which 624,493 events concern movements (Fig. 2.1(b)) and 4,845,546 events are demographic. This type of data is commonly recorded for livestock populations in many countries (Brooks-Pollock et al., 2014a), and is here relied upon to connect the nodes by a transport network such that the overall spread mechanism is of *hybrid* character (Zhang et al., 2015).

Without limiting the generality of the discussion, epidemiological measurements can be regarded as a filter operating on the full epidemiological state. In our case this filter simply returns a binary answer 0 or 1 *per node*: infection not detected/detected, and we assume that a probabilistic model for this response is available and can be simulated *in silico* as a black box. The available observations of STEC O157 were collected from a subset of 126 nodes on a bi-monthly basis during the time frame 2009–2012 (Widgren et al., 2015), and the results were aggregated per quarter year, see Fig. 2.1(c). Each observation included several bacteriological samples from the farm environment resulting in a negative or positive detection per node. To truthfully mimic this *in silico* we rely on an urn model driven by empirically known sensitivities given an underlying node prevalence. Details concerning the pathogen detection protocol and the associated urn model are found in the Supporting Information (SI).

2.3. Approximate Bayesian computations

The simulation-driven Bayesian setup can be summarized as follows. We regard the epidemiological model as a stochastic process $X_t = X_t(\theta)$ in continuous time, dependent upon some parameter $\theta = [\theta_1, \theta_2, \dots]$. Data from this process is collected via some measurement filter $M(\cdot)$ operating on the state of the process at time t_i , i.e., $x_i = M(X(t_i; \theta))$, and where the filter itself might be an additional source of noise. We assume that there is a simulator $F(\cdot)$ that simulates *and* measures the process such that data may be sampled *in silico* provided that a parameter value θ is proposed, e.g., $z \sim F(\theta)$ simulates new data $z = (z_i)$. The likelihood $\mathbf{P}(\cdot|\theta)$ is generally computationally intractable, although in principle the problem can be formulated as a missing data problem (see e.g. (Lau et al., 2017)), these are typically very computationally intensive and difficult to implement. Instead, an alternative approach is to use simulation-driven approximate Bayesian methods which find an approximate posterior distribution.

The basic ABC rejection sampler (Beaumont et al., 2002) accepts proposed parameters depending on the output from a kernel function $K_\varepsilon(\|z - x\|)$ with distance $\varepsilon \geq 0$. A common approximation step is the use of *summary statistics* $s = S(z)$, effectively reducing the dimensionality of the data to compare; instead of measuring the distance between the full data, one uses the summary statistics of the data. The probability that we accept a parameter proposal from a prior $\theta' \sim P(\theta)$ is then given by $K_\varepsilon(\|S(z) - S(x)\|)$ where $z \sim F(\theta')$. The problem of choosing suitable summary statistics is discussed in (Sisson et al., 2018, Chap. 5). We select our summary statistics similarly to previous suggestions for systems of comparable seasonal characteristics (Papamakarios and Murray, 2016; Everitt, 2018). The statistics we use for our data, a time series of the number of aggregated positive samples per quarter year, are the mean prevalence per quarter and the two largest in magnitude Fourier coefficients, all in all 6 summarizing statistics coefficients.

For observed summary statistics $s_{\text{obs}} = S(x)$, the resulting ABC posterior, $\mathbf{P}_{\text{ABC}}(\theta|s_{\text{obs}})$, has the form

$$\mathbf{P}_{\text{ABC}}(\theta|s_{\text{obs}}) \propto \int K_\varepsilon(\|s - s_{\text{obs}}\|) \mathbf{P}(s|\theta) P(\theta) ds, \quad (2.3)$$

where $\mathbf{P}(s|\theta)$ is the likelihood of $s = S(z)$ implied by $\mathbf{P}(z|\theta)$. If $\varepsilon \rightarrow 0$, then by the properties of the kernel function, $\lim_{\varepsilon \rightarrow 0} \mathbf{P}_{\text{ABC}}(\theta|s_{\text{obs}}) \propto \mathbf{P}(s_{\text{obs}}|\theta) P(\theta)$. Hence the posterior is exact provided the summary statistics are sufficient, i.e., that no information is lost (Sisson et al., 2018, Chap. 1). However, this is commonly not the case and the ABC posterior is then only approximate.

2.4. Adaptive Markov chain Monte Carlo and synthetic likelihoods

A downside of ABC rejection is its comparably low acceptance rate. Successful attempts to address this have been achieved by combining the ABC methodology with existing likelihood-based sampling methods, e.g., Metropolis-Hastings (Marjoram et al., 2003). In the seminal work (Wood, 2010), it was observed that measured summary statistics are often asymptotically normally distributed, i.e., $s \sim \mathcal{N}(\mu, \Sigma)$ with mean μ and covariance Σ . The (limiting) likelihood of the observed summary statistic is then the probability $\mathcal{N}(s_{\text{obs}}|\mu, \Sigma)$, usually referred to as the synthetic likelihood (SL). Since μ and Σ are not known they must be estimated, and a natural idea is to replace them by sample estimates from multiple simulations of z with the same proposal θ^* :

$$\mathbf{S} = (S_i) = (S(z_1), S(z_2), \dots, S(z_N)), \quad z_j \sim F(\theta^*), \quad (2.4)$$

$$\hat{\mu} = \frac{1}{N} \sum_{i=1}^N S_i, \quad (2.5)$$

$$\hat{\Sigma} = \frac{1}{N-1} \sum_{i=1}^N (S_i - \hat{\mu})(S_i - \hat{\mu})^\top, \quad (2.6)$$

for which the log-SL is

$$\log \mathcal{N}(s_{\text{obs}}|\hat{\mu}, \hat{\Sigma}) = -\frac{1}{2}(s_{\text{obs}} - \hat{\mu})^\top \hat{\Sigma}^{-1} (s_{\text{obs}} - \hat{\mu}) - \frac{1}{2} \log |\hat{\Sigma}| - \frac{N \dim(s)}{2} \log(2\pi). \quad (2.7)$$

Now consider the SL as $N \rightarrow \infty$. Under broad assumptions (2.5) and (2.6) will converge to (μ, Σ) . However, the limit can be computationally impractical for models which are expensive to simulate. An approach to improve the estimate of SL is by using the bootstrap (Efron, 1979), and (Everitt, 2018) recently proposed an empirical bootstrapping procedure designed specifically for SL-driven algorithms. We found that it successfully produced more robust estimates of the SL using fewer model calls. The idea is to first determine an empirical distribution $\hat{\mathbf{F}}_N(\theta^*)$ by using N independent simulations as follows. We compute synthetic data (z_{ij}) , where $i = 1, \dots, N_{\text{time}}$ runs over time as before and $j = 1, \dots, N$ runs over the number of independent trajectories used. Notably, the empirical distribution is a distribution over $\mathbf{R}^{N_{\text{time}}}$ and is constructed by assuming each trajectory to yield N_{time} independent samples, one per each point in time. While this assumption is not exactly fulfilled, the measurements are well separated in time such that independence should be at least an accurate approximation.

From the empirical distributions, we next sample $R \gg N$ new such time series by iterating through the N_{time} time points, independently sampling with replacement from each of the N recorded simulated trajectories, and building up in this way each sampled time series. The use of the bootstrap scheme thus results in a larger dataset, effectively bootstrapping the estimate closer to the desired limit of $N \rightarrow \infty$. Practically, the sample sizes used in our experiments were $N = 20$ and $R = 100$.

The SL can be used in any desired likelihood-based inference method. We chose to implement the SL in an Adaptive Metropolis (AM) scheme (Haario et al., 2001). Instead of sampling proposals from a fixed prior distribution, the AM scheme samples adaptively using a Gaussian with covariance matrix computed from the previous entries in the

Markov chain (Haario et al., 2001),

$$C_{i+1} = \frac{i-1}{i} C_i + \frac{\xi_d}{i} (i\tilde{\theta}_{i-1}\tilde{\theta}_{i-1}^T - (i+1)\tilde{\theta}_i\tilde{\theta}_i^T + \theta_i\theta_i^T + \epsilon I_d), \quad (2.8)$$

which does not add significant computational time, since the running mean of the chain $\tilde{\theta}_i$ can be computed recursively. In (2.8), ξ_d is a tuning parameter for the proposal distance, as in regular Metropolis (Metropolis et al., 1953), and one uses a small value ϵ to prevent a possible degeneration of C_i . The adaptivity results in the loss of the Markov property between samples, however, the chain keeps the desired ergodic properties of its non-adaptive counterpart (Haario et al., 2001; Andrieu and Moulines, 2006).

We refer to the combined algorithm as Bootstrapped Synthetic Likelihood Adaptive Metropolis (SLAM) (Algorithm 1).

Algorithm 1. Synthetic Likelihood Adaptive Metropolis (SLAM).

Require: Summarized data s_{obs} and initial guess $(\theta_1, \mathcal{L}_\theta)$. Adaptivity parameters i_0, C_0, ξ_d , and ϵ (see text for details).

```

1:   for  $i = 2, \dots, N_{\text{sample}}$  do
2:     if  $i > i_0$  then Compute  $C_i$  by (2.8) else  $C_i = C_0$ 
3:     Sample  $\theta^* \sim N(\theta_{i-1}, C_i)$ 
4:     Simulate  $Y = (y_1, \dots, y_N), y_j \sim F(\theta^*)$ 
5:     Bootstrap  $Z = (z_1, \dots, z_R), z_j \sim \hat{F}_N(Y)$ 
6:     Estimate  $(\hat{\mu}_{\theta^*}, \hat{\Sigma}_{\theta^*})$  from  $S = S(Z)$ , with (2.5) and (2.6)
7:     Compute  $\mathcal{L}_{\theta^*} = \mathbf{P}_{\theta^*}(s_{\text{obs}}|S)$  by (2.7)
8:     if  $\text{Uniform}(0, 1) < \min(1, \mathcal{L}_{\theta^*}/\mathcal{L}_\theta)$  then
9:        $\theta_i = \theta^*$  and  $\mathcal{L}_\theta = \mathcal{L}_{\theta^*}$ 
10:    else
11:       $\theta_i = \theta_{i-1}$ 

```

After running the adaptive Metropolis sampler for N_{train} proposals using P independent parallel replicas, all with independent initial starting points, the AM has explored the support of the posterior. To refine the sample resolution, we next deploy a Metropolized Independent Sampler (MIS) (Hastings, 1970), for N_{sample} proposals, again running in P independent parallel replicas. These replicas all use a single static normal proposal density, namely the aggregate of the training replicas (mean of normal means and covariances after removal of a burn-in transient). The use of a MIS lowers the correlation between samples and shortens the burn-in time. Additionally, using a prior adapted proposal distribution, the MIS sample rate is more resource efficient than the training phase. This scheme of combining AM and MIS is reminiscent of the block-adaptive strategy proposed in Jacob et al. (2011), however, without any further adaptation after the first block, see Algorithm 2 in the SI.

2.5. Parametric bootstrap and estimator efficiency

The target of a Bayesian approach to parameterization is the parameter posterior distribution \mathbf{P}^* and its samples $\theta^* \sim \mathbf{P}^*$. In practice, the best one can hope for is approximate posterior samples $\tilde{\theta} \sim \tilde{\mathbf{P}}$, obtained from a numerical model which approximates the processes underlying the data, and using some approximate posterior sampling procedure. The error in the Bayesian posterior estimator is then formally the difference $\tilde{E} := \tilde{\theta} - \theta^*$, but without any useful dependency relation between \mathbf{P}^* and $\tilde{\mathbf{P}}$, one in practice seeks to quantify some statistics of this error. Useful such measures are typically derived from a point estimator of θ^* and we consider the minimum mean square error estimator (MMSE) for this purpose, which is just the mean of the true posterior, $\theta^* := E[\theta^*]$. The mean square error is then

$$\tilde{e}^2 := E[(\tilde{\theta} - \theta^*)^2] = \underbrace{E[(\tilde{\theta} - E[\tilde{\theta}])^2]}_{\text{Variance}} + \underbrace{(E[\tilde{\theta}] - \theta^*)^2}_{\text{Square bias}}, \quad (2.9)$$

where $\tilde{\theta} := E[\tilde{\theta}]$ is the MMSE of $\tilde{\theta}$. This decomposes the mean square error into the variance of $\tilde{\theta}$ and the square of the bias

$$\tilde{b} := E[\tilde{E}] = \tilde{\theta} - \theta^*.$$

The procedure we propose for estimating the bias falls under the class of methods referred to as *parametric bootstrap* (Efron, 1979). The general idea is to treat inference about \mathbf{P}^* for the original data as comparable to inference of $\tilde{\mathbf{P}}$ for resampled synthetic data. We thus use the same Bayesian posterior sampling used to sample from $\tilde{\mathbf{P}}$ a second time and produce samples $\tilde{\theta} \sim \tilde{\mathbf{P}}$, that is, from the posterior given synthetic data generated from known parameters. The synthetic data may be generated by either parameters drawn from $\tilde{\mathbf{P}}$, or from an associated point estimator. We simply used the MMSE for this step and generated data using the sample mean from the posterior $\tilde{\mathbf{P}}$, that is, for $\tilde{\theta} := N_{\text{sample}}^{-1} \sum_i \tilde{\theta}_i$, where $(\tilde{\theta}_i)$ are samples from $\tilde{\mathbf{P}}$. The error in this data-synthetic inference is $\tilde{\tilde{E}} := \tilde{\theta} - \hat{\theta}$, and hence its bias is $\tilde{\tilde{b}} := E[\tilde{\tilde{E}}]$, readily estimated as a sample mean. The bootstrap estimate of the wanted bias is then simply $\tilde{b} \approx \tilde{b}_{\text{BS}} := \tilde{\tilde{b}}$, which together with the sample variance of $(\tilde{\theta}_i)$ yields the bootstrap estimate of the mean square error as in (2.9).

For our data we generated $M_{\text{boot}} = 10$ posterior distributions $\tilde{\mathbf{P}}$ using independent model data realizations from the same parameter $\hat{\theta}$. Each distribution consisted of $N_{\text{sample}} = 45$ samples, after removal of burn-in (= 500) and thinning (every 100th). Finally, the estimated bias was computed as the average bias across the M_{boot} bootstrap posteriors.

3. Results

We first look into the issue of the model's identifiability by working through a set of synthetic set-ups on smaller scale using known-truth data. The rationale here is that, if this phase does not succeed, there will be little hope in coping with more realistic situations. Results on this are reported in Section 3.1 where, as a side-effect, we also quantify the efficiency of the SLAM compared to the basic ABC rejection procedure. Our main results are found in Section 3.2 where a full national scale STEC O157 model based on first principles is parameterized from available pathogen data. Applications concerning detection and intervention scenarios are exemplified in Sections 3.3 and 3.4.

3.1. Identifiability and the efficiency of SLAM

Given real-world pathogen data and a disease spread model with an intractable likelihood, the options to rigorously analyze the parameters' identifiability are quite limited. A practical approach is to evaluate how well a proposed inference method performs on synthetic data drawn from a known model. By testing different inference procedures on a problem with an established truth and comparing their estimation qualities, we empirically reveal both identifiability and estimator efficiency. In the Bayesian setting we may, for example, compare the error in some point estimator derived from the posterior, e.g., the average of the posterior samples (the minimum mean square error estimator). If the stability of the inference procedure remains when confronted with real data, then we may use the bootstrap procedure discussed in Section 2.5 to more rigorously assess the quality of the posterior.

Our full scale national model is computationally expensive, particularly so considering that parameterization requires large quantities of sample trajectories. To more effectively explore the limits of the methodology, we initially consider a synthetic set-up at a smaller scale. We define this scaled down model over 1600 nodes, using synthetically generated movements of individuals for four years while recording the full epidemiological state every 60th day on a sample of 100 randomly chosen nodes (see the SI for details on how this was done in practice). We now ask if this synthetic data can be used to reliably infer the parameters used in the local infection model: ν, β , and γ . We artificially construct some seasonality by using two values of β , that is, β_1 and β_2 each cover a 6-month period of the year, and we consider this modeling choice to be part of the prior information together with precise knowledge of the initial state at time $t = 0$. This synthetic set-up is fast

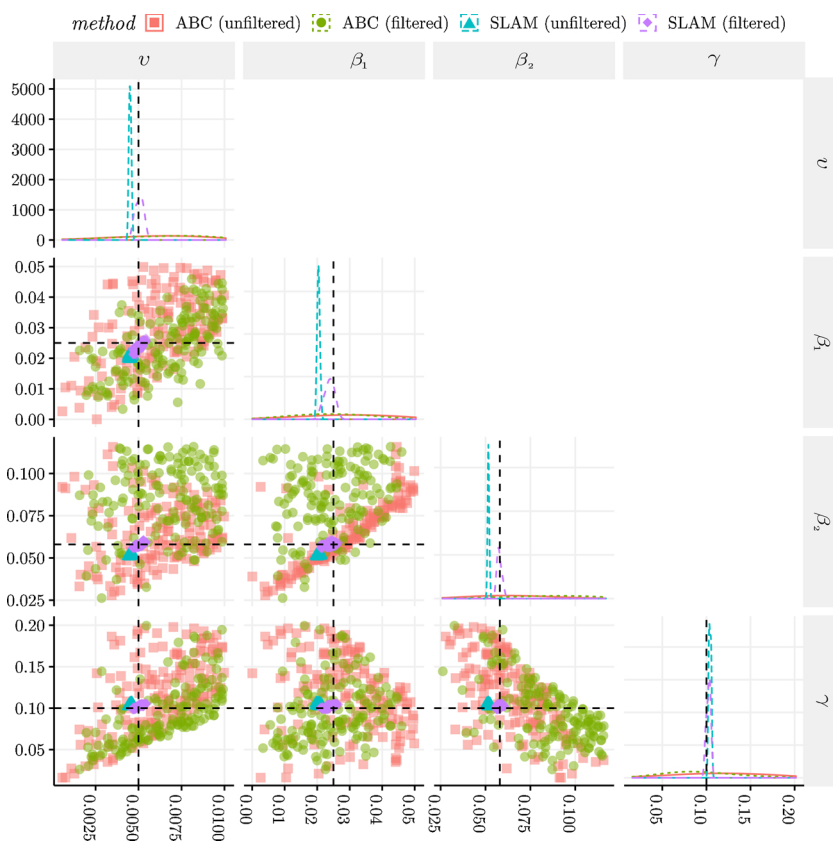


Fig. 3.1. Posterior samples for the 1600 nodes synthetic dataset (positive uniform unnormalized priors). The samples, indicated by distinct colors and shapes, are generated by either ABC rejection (on unfiltered & binary filtered data) or SLAM (on unfiltered & binary filtered data). The true parameters are indicated by the horizontal and vertical black & dashed lines. For comparable results both methods were run the same amount of wall-clock time. The plots on the diagonal are the marginal posterior distribution per parameter. The lower diagonal plots are bi-dimensional posterior samples. The axis show the parameter values, except for the top left plot's y-axis which is the density. (For interpretation of the references to color in this figure legend, the reader is referred to the web version of this article).

to simulate but preserves many of the main characteristics of the full national scale model.

We supply this system with parameters which, after some initial trial and error, were found to be reasonably close to the domain of relevance for the STEC O157 application later considered. Data from a single simulation was fed into an off-the-shelf ABC rejection sampler as well as into our own SLAM posterior sampler. The procedures were initially given “unfiltered” data in the form of the exact disease prevalence, i.e. the fraction of infected individuals, at the 100 selected nodes and at the sample points in time. Later, we moved on to *binary filtered* data obtained by subjecting the full state to a computational model of a certain pathogen detection protocol, see the discussion in Section 2.2 with further details in the SI (cf. also Fig. 2.1(c)). Intuitively, one expects a hopefully acceptable loss of estimator accuracy when switching to filtered data.

The resulting posteriors are shown in Fig. 3.1. All samplers were successful in this synthetic setting. For SLAM, filtering the data implies a small increase in posterior width, and a minor improvement of the mean posterior bias. Although the effect in bias is a bit surprising, the difference is quite small and, moreover, a shift in bias is suitable to handle through bootstrapping estimates as is done in Section 3.2. The quality of the ABC sampler is somewhat more difficult to assess. Since unfiltered data is a best possible scenario, this case also defines an upper bound of the posterior quality. For the ABC sampler, the filtered state observations yield a posterior which is seemingly unaffected by the data being filtered. Since proposals are accepted under an ϵ -criterion, and since with different kinds of data, the meaning of ϵ varies, the unfiltered and filtered versions cannot be directly compared. Perhaps more interestingly, the error of the SLAM MMSE estimator is almost one order of magnitude smaller than that of the corresponding ABC-estimator (see the SI for exact errors), conditioned on using the same amount of wall-clock time. These results show that the transition from a straightforward ABC rejection sampler to a posterior obtained via a synthetic likelihood ansatz can pay off well.

3.2. National scale Bayesian inversion

As we now show, SLAM is successful in inverting a full national scale model of the spread of STEC O157 using the pathogen data from (Widgren et al., 2015). We consider anew the SIS_E model in Fig. 2.1(a), now replicated across 37,220 actual nodes (herds) populated by about 1.6 million individual animals, and connected by the full eight year national scale animal movement dataset over Sweden (Fig. 2.1(b)). The model parameters are $(v, \beta_1, \beta_2, \beta_4, \gamma, p_0)$, where $(\beta_{1,2,3,4})$ is the decay of infectious matter for [spring, summer, fall, winter], and $\beta_1 = \beta_3$ to simplify. As mentioned, seasons were inferred on a per-node basis using climate data from the Swedish Meteorological and Hydrological Institute. The parameter p_0 is a compact description of the system's initial state as follows. On initialization the total number of individuals $S_0 + I_0$ at each node is known from data, and we first sample I_0 to match any proposed prevalence p_0 : $I_0/(S_0 + I_0) \approx p_0$. Effectively assuming equilibrium ($\varphi'(0) \approx 0$ in (2.2)), we next set the node's initial environmental infectious pressure to be $\varphi_0 = \beta^{-1}I_0/(S_0 + I_0)$.

The pathogen data from Widgren et al. (2015) is understood as the result of the binary filter applied to the full state of the tested node. The measures are low-informative on the epidemiological state and distributed sparsely in both space and time: about 6–8 binary true/false samples per year, and only at 0.3% of the nodes. The computational complexity is a significant difficulty of any realistic inverse problem. For each parameter proposal, we estimate the synthetic likelihood from $N = 20$ trajectories, bootstrapped to $R = 100$. One trajectory results from about 10^8 simulated events such that, in the end, each proposal is evaluated in about 60s over 16 compute cores ($2 \times$ Intel Xeon E5-2660). Similar to the inversion of the 1600 node network in Section 3.1, before using any real observations, we tested the feasibility using synthetic known-truth observations.

We obtain the approximate posterior parameter distribution of the STEC O157 endemics in Fig. 3.2. We next perform parametric bootstrap as discussed and improve on our confidence in the results by

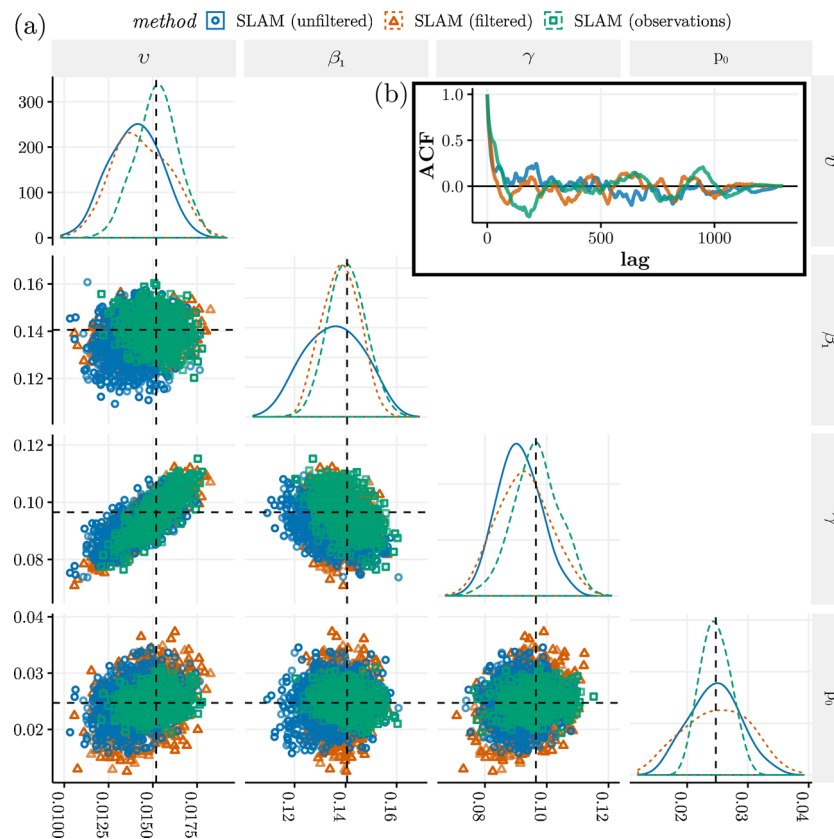


Fig. 3.2. (a) Posterior parameter samples obtained from SLAM given synthetic unfiltered data, binary filtered data, and real pathogen observations (positive uniform unnormalized priors). The multivariate Gelman and Rubin's convergence diagnostic for each method is [1.05, 1.09, 1.07]. A version of the figure including all β dimensions is found in the SI. The horizontal and vertical black & dashed lines are the MMSE estimators from SLAM (observations): $(v, \beta_1, \gamma, p_0) = (0.0151, 0.141, 0.0965, 0.0247)$. (b) The autocorrelation of the samples from one of the parallel chains of the parameter v .

leveraging the stability of the inference procedure as follows. The posterior mean is used as a suitable parameter to replicate new synthetic data for, and the inference procedure is put to work again using this data. Here we apply SLAM both to the synthetic unfiltered data as well as to the filtered version. As seen in Fig. 3.2 the posterior distributions all match very closely. We quantify the accuracy of the minimum mean square error (MMSE) parameter point estimator through the MSE for the three posteriors. The bias is unknown for the most interesting case of real observations and we there have to impute the bias via the corresponding synthetic quantities, resulting in a bootstrapped/imputed estimated accuracy of the point estimator (Efron, 1979). All MMSE parameter estimators were found to be within 10% accuracy and in most cases within 5% (see SI).

The posterior fit to data can be judged by comparing our estimated node prevalence of 11.2[7.9, 15.5]%, at 95% credible interval (CI) from $N = 250$ posterior parameters, to the reported value 13.1% (Widgren et al., 2015). We further validated our posterior by looking at two independent observational studies. We estimated the temporal population prevalence to 2.2[1.5, 3.5]% for (2008–09) and, respectively, to 2.2[1.5, 3.3]% (2011–12) ($N = 250$, 95% CI). These measures compare well to the studies (European Food safety authority and European Centre for Disease Prevention and Control, 2012, 2014), where those figures are 3.3% and 3.1%, respectively. In Fig. 3.3 the posterior simulator is also compared more directly to data.

For the parameters, our accuracy can be summarized as an average coefficient of variation of around 7%, while previous comparable attempts obtain around 30% (Ferguson et al., 2003, 2005; Fournié et al., 2018; Merler et al., 2011; Brouwer et al., 2018; Brooks-Pollock et al., 2014b), albeit in most cases for point estimators (a notable exception is (Brooks-Pollock et al., 2014b), which also fit a stochastic national scale

livestock disease model incorporating movement data within a Bayesian (ABC) framework). From our experience, the most decisive steps towards the quality of our results were (1) the good topological agreement in the prior model formulation through the combined effects of detailed network data and a local climate-dependent β , (2) the effective parameterization of the initial state through the scalar p_0 , and (3), the use of empirical bootstrapping to increase the robustness in estimating the synthetic likelihood. Additionally, using adaptive Metropolis proposals increased the sampling efficiency considerably.

3.3. Detection: large nodes are nearly optimal sentinels

The number of human STEC O157 cases is less than about 10 per 100,000, but the risk for children is considerably higher than for adults. Infected individuals often develop bloody diarrhea, and about 5–10% further develop hemolytic-uremic syndrome, a severe complication that can be fatal (Parry and Palmer, 2000). By reviewing surveillance routines and mitigation strategies, one could reduce the prevalence of STEC O157 in reservoirs, e.g., in the cattle population, thus potentially reducing the number of human infections (Bajardi et al., 2012; Widgren et al., 2016; Keeling et al., 2017). The process of selecting sentinel nodes has been actively studied (Keeling and Eames., 2005; Bajardi et al., 2012; Schärer et al., 2015), and here we propose a way by which the sensitivity of the pathogen detection procedures can be improved within our framework.

We test five different kinds of *sentinel* node sets, each of the same size (10 nodes), and evaluate their detection sensitivity through multiple simulations, using $N = 250$ sample parameters from the previously computed parameter posterior. The first four sets are defined in terms of simple network measures, namely indegree (Indegree), outdegree

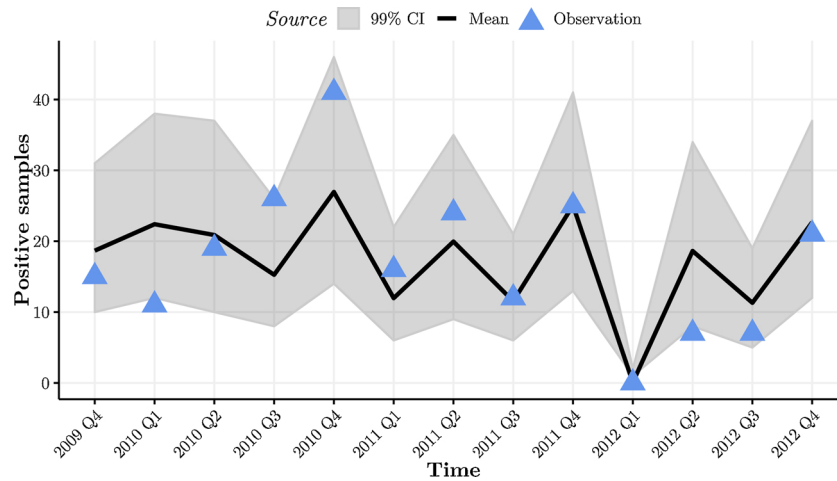


Fig. 3.3. Posterior predictive check: the observations of the full system and $N = 2000$ posterior sample trajectories. The blue triangles are the observations of the number of aggregated positive samples per quarter, the solid black line is the mean of the posterior samples and the shaded area is the 99% credible interval. (For interpretation of the references to color in this figure legend, the reader is referred to the web version of this article).

(Outdegree), node population (Largest), and, for reference, a random set (Random). We design the fifth set (Observation) to be nearly optimal as follows. We first simulated independent trajectories for eight years, while recording the infectious pressure φ during the final four years. By ranking the nodes in the system according to the environmental pathogen load φ , we obtained a shortlist of the 10 most infected nodes, and we let these serve as a close to optimal detection set of nodes.

For the evaluation of the node detectability, the system is simulated using parameters from the posterior distribution. We define the detection sensitivity for the sentinel nodes by using a simple detection probability model as follows. At node set N_i and at time t , compute $P(\text{detect infection}) = 1 - \prod_{i \in N_i} (1 - P_i(\varphi_i(t)))$, where $P_i(\cdot)$ is modeled by a sigmoid function, $P_i(x) = 1/[1 + \exp(-k(x - \varphi_0))]$, where k is the test's sharpness and φ_0 the cut-off. Although our choice of sigmoid parameters is not important for our purposes and were arbitrary, the modeling choices here can clearly be made to mimic any empirically known sensitivity.

The measured detection probability, displayed in Fig. 3.4, shows that the node set *Largest* is about as efficient as the upper limit estimate *Observation*. An explanation for the apparent efficiency of population size as a priority measure for detection procedures lies in the *rescue effect* (Keeling and Rohani, 2008), which states that, in a metapopulation with high interconnectivity, the larger nodes take the role of “rescuing” the disease from extinction; an early observation of this phenomenon was made in (Finkenstädt et al., 2002) in a study of

measles. The largest nodes tend to remain continuously infected such that the infectious pressure is larger than elsewhere. This is also consistent with large groups of cattle being more likely to be STEC positive (Vidovic and Korber, 2006; Ellis-Iversen et al., 2007). The marginal performance differences between sets based on outdegree and indegree is in line with previous findings (Bajardi et al., 2012), that is, they do not show a significant improvement to using randomly selected nodes. Note also the clear periodic trend which could well be exploited to propose further refined detection strategies.

3.4. Intervention: best results from local actions

An important purpose with a computational epidemiological framework is to assess the effects of interventions. In (Merler et al., 2015; Peak et al., 2017) the efficiency of mitigation strategies for epidemics were evaluated using data-driven agent-based models, and a Bayesian node-based framework was employed for the same purpose in (Brooks-Pollock et al., 2014b). For STEC O157, (Widgren et al., 2018) proposes and assesses various interventions, although not in a probabilistic framework. We test comparable intervention proposals in our Bayesian *in silico* model.

We sample 250 model parameters from the posterior and simulate for four years to avoid any transient effects. Then we intervene according to three strategies as follows. The first strategy is to remove transmission by transport, i.e., if an infected animal is moved we change the status to susceptible on arrival. The second strategy is to

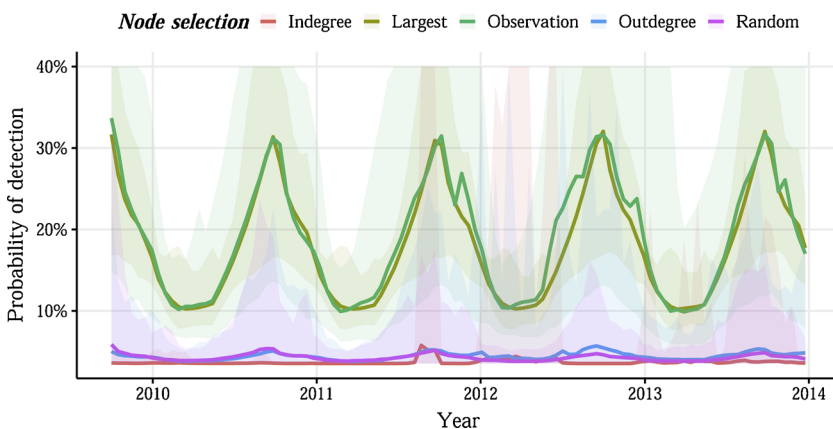


Fig. 3.4. The detection probability over time for five different sets of sentinel nodes. The node sets *Indegree*, *Largest*, and *Outdegree* were defined from basic network statistics, and *Random* using uniform node sampling. The *Observation* set is found through pre-simulation and is nearly optimal. Each set included the 10 highest ranking nodes according to each criterion. Displayed is the mean detection probability and 95% CI. Sigmoid model parameters: $k = 15$ and $\varphi_0 = 0.375$, for which $\varphi \in [0.13, 0.62]$ forms a symmetric 95% CI.

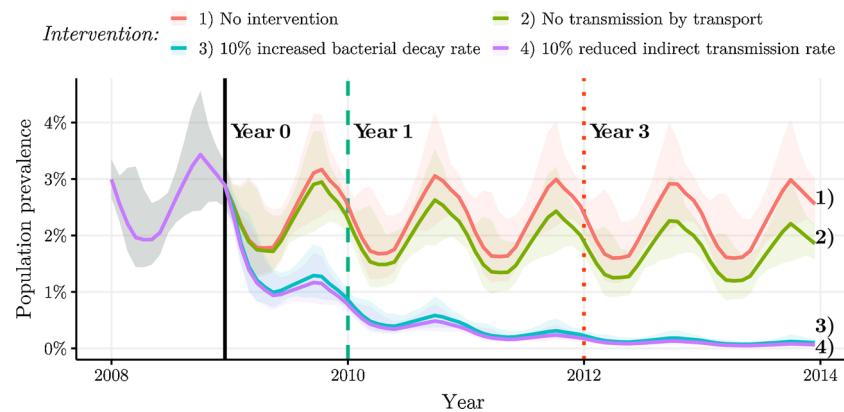


Fig. 3.5. The prevalence response to intervention. Three different techniques were tested starting from the intervention point in time (solid vertical line). Displayed is the mean population prevalence and 95% CI. Measured reduction rates for each intervention protocol are reported in the SI.

increase the bacterial decay rate β by 10%, and the third is to reduce the indirect transmission rate ν by 10%. These interventions do not invalidate the recorded transport events and therefore do not interfere with any implicit causality. After the selected intervention we record the population prevalence for five more years.

In line with the results of Widgren et al. (2018), in Fig. 3.5 we conclude that control strategies that emphasize local intervention apparently give the best results, as after three years the infection is controlled. Although the precise interpretation of the local strategies needs to be defined, the relative effects on the parameters could in principle be estimated through experiments with practical procedures including, e.g., improved on-farm biosecurity or vaccination.

4. Discussion

Epidemiological models have both qualitative and quantitative applications, and different trade-offs clearly apply depending on the purpose of the model (Ferguson et al., 2003; Keeling and Rohani, 2008). In this paper we emphasized computational models designed with the goal of assessing large-scale disease spread in a quantitative sense. This is the regime of models for which data is essential (Merler et al., 2015; Liu et al., 2018; Walters et al., 2018), both in driving the model, e.g., detailed network data in our case, but also in parameterizing the model using surveillance measurements. Given that pathogen surveillance data is likely to become cheaper and more accessible, e.g., with improvements in biosensors for livestock (Vidic et al., 2017), data-driven models could facilitate timely and effective response to various infections.

We have demonstrated the feasibility of a Bayesian parameterization on a national scale using field data from the spread of STEC O157 in Swedish cattle. The main modeling assumptions are that network data is available and that the pathogen detection procedure can be replicated *in silico*. The use of a detailed transport pattern facilitates model inversion thanks to the high level of topological agreement already in the prior model formulation. For weakly informative pathogen detection protocols, we developed ideas on approaching the question of parameter identifiability via a series of controlled synthetic data experiments. Our findings here support the use of synthetic likelihoods and an adaptive Metropolis sampling over the more straightforward ABC sampler. Once parameters have been identified, parametric bootstrap enables an estimation of the confidence in the inference procedure.

With the methodology developed here a substantial improvement in the qualities of surveillance and control procedures in animal and public health is possible. We have exemplified this in the ranking of detection- and intervention procedures, where detailed credible bounds are directly available thanks to the Bayesian framework. Our work opens up the potential for better use of quantitative large-scale

epidemiological models whenever sufficient data is available. With the increasing amounts of epidemiologically relevant data being collected, we conclude that there is also an important role to be played by models consistently driven by and informed from this data.

Authors' contributions

SE conceived the research with inputs from SW. SE and RE developed the methodology and the experiments, and RE carried out the implementations. SW prepared animal- and pathogen data and SE and SW developed the *SimInf* epidemiological simulation framework. The paper was drafted by the two first authors and revised by all authors.

Funding

This work was financially supported by the Swedish Research Council Formas (S. Engblom, S. Widgren), by the Swedish Research Council within the UPMARC Linnaeus center of Excellence (S. Engblom, R. Eriksson), and by the Swedish strategic research program eSENCE (S. Widgren). The simulations were performed on resources provided by the Swedish National Infrastructure for Computing (SNIC) at UPPMAX.

Conflict of interest

The authors declare that there is no conflict of interests.

Appendix A. Supplementary data, modeling, and computational protocols

Supplementary data associated with this article can be found, in the online version, at <https://doi.org/10.1016/j.epidem.2020.100399>.

References

- Anderson, R.M., May, R.M., 1981. The population dynamics of microparasites and their invertebrate hosts. *Philos. Trans. R. Soc. Lond. B Biol. Sci.* 291 (1054), 451–524. <https://doi.org/10.1098/rstb.1981.0005>.
- Andrieu, C., Moulines, É., 2006. On the ergodicity properties of some adaptive MCMC algorithms. *Ann. Appl. Probab.* 16 (3), 1462–1505.
- Bajardi, P., Barrat, A., Savini, L., Colizza, V., 2012. Optimizing surveillance for livestock disease spreading through animal movements. *J. R. Soc. Interface* 9 (76), 2814–2825.
- Balcan, D., Colizza, V., Gonçalves, B., Hu, H., Ramasco, J.J., Vespignani, A., 2009. Multiscale mobility networks and the spatial spreading of infectious diseases. *Proc. Natl. Acad. Sci. USA* 106 (51), 21484–21489.
- Beaumont, M.A., Zhang, W., Balding, D.J., 2002. Approximate Bayesian computation in population genetics. *Genetics* 162 (4), 2025–2035.
- Brooks-Pollock, E., de Jong, M., Keeling, M., Klinkenberg, D., Wood, J., 2014a. Eight challenges in modelling infectious livestock diseases. *Epidemics* 10 (1–5). <https://doi.org/10.1016/j.epidem.2014.08.005>.
- Brooks-Pollock, E., Roberts, G.O., Keeling, M.J., 2014b. A dynamic model of bovine tuberculosis spread and control in Great Britain. *Nature* 511, 228.
- Brouwer, A.F., Eisenberg, J.N., Pomeroy, C.D., Shulman, L.M., Hindiyyeh, M., Manor, Y.,

- Grotto, I., Koopman, J.S., Eisenberg, M.C., 2018. Epidemiology of the silent polio outbreak in Rahat, Israel, based on modeling of environmental surveillance data. *Proc. Natl. Acad. Sci. USA* 115 (45), E10625–E10633.
- Degli Atti, M.L.C., Merler, S., Rizzo, C., Ajelli, M., Massari, M., Manfredi, P., Furlanello, C., Tomba, G.S., Iannelli, M., 2008. Mitigation measures for pandemic influenza in Italy: an individual based model considering different scenarios. *PLoS ONE* 3 (3), e1790.
- Efron, B., 1979. Bootstrap methods: another look at the jackknife. *Ann. Stat.* 7.
- Ellis-Iversen, J., Smith, R.P., Snow, L.C., Watson, E., Millar, M.F., Pritchard, G.C., Sayers, A.R., Cook, A.J., Evans, S.J., Paiba, G.A., 2007. Identification of management risk factors for VTEC O157 in young-stock in England and Wales. *Prev. Vet. Med.* 82 (1–2), 29–41.
- Engblom, S., Widgren, S., 2017. Data-driven computational disease spread modeling: from measurement to parametrization and control. In: Rao, C.R., Rao, A.S., Payne, S. (Eds.), *Disease Modeling and Public Health: Part A, Volume 36 of Handbook of Statistics*. Elsevier, Amsterdam, pp. 305–328. <https://doi.org/10.1016/bs.host.2017.05.005>. chapter 11.
- Eubank, S., Guclu, H., Kumar, V.A., Marathe, M.V., Srinivasan, A., Toroczkai, Z., Wang, N., 2004. Modelling disease outbreaks in realistic urban social networks. *Nature* 429 (6988), 180.
- European Food safety authority and European Centre for Disease Prevention and Control, 2012. The European union summary report on trends and sources of zoonoses, zoonotic agents and food-borne outbreaks in 2010. *EFSA J.* 10 (3), 2597. <https://doi.org/10.2903/j.efsa.2012.2597>.
- European Food Safety Authority and European Centre for Disease Prevention and Control, 2014. The European union summary report on trends and sources of zoonoses, zoonotic agents and food-borne outbreaks in 2012. *EFSA J.* 12 (2), 3547. <https://doi.org/10.2903/j.efsa.2014.3547>.
- Everitt, R.G., 2018. Bootstrapped Synthetic Likelihood. (Preprint), (posted 17.01.18). [arXiv:1711.05825v2](https://arxiv.org/abs/1711.05825v2).
- Ferguson, N.M., Keeling, M.J., Edmunds, W.J., Gani, R., Grenfell, B.T., Anderson, R.M., Leach, S., 2003. Planning for smallpox outbreaks. *Nature* 425 (6959), 681.
- Ferguson, N.M., Cummings, D.A., Cauchemez, S., Fraser, C., Riley, S., Meeyai, A., Iamsrithaworn, S., Burke, D.S., 2005. Strategies for containing an emerging influenza pandemic in southeast Asia. *Nature* 437 (7056), 209.
- Finkenstädt, B.F., Bjørnstad, O.N., Grenfell, B.T., 2002. A stochastic model for extinction and recurrence of epidemics: estimation and inference for measles outbreaks. *Biostatistics* 3 (4), 493–510.
- Fournié, G., Waret-Szkuta, A., Camacho, A., Yigezu, L.M., Pfeiffer, D.U., Roger, F., 2018. A dynamic model of transmission and elimination of peste des petits ruminants in Ethiopia. *Proc. Natl. Acad. Sci. USA* 115 (33), 8454–8459.
- Germann, T.C., Kadau, K., Longini, I.M., Macken, C.A., 2006. Mitigation strategies for pandemic influenza in the United States. *Proc. Natl. Acad. Sci. USA* 103 (15), 5935–5940.
- Haario, H., Saksman, E., Tamminen, J., 2001. An adaptive Metropolis algorithm. *Bernoulli* 7 (2), 223–242.
- Hastings, W.K., 1970. Monte Carlo sampling methods using Markov chains and their applications. *Biometrika* 57, 97–109.
- Jacob, P., Robert, C.P., Smith, M.H., 2011. Using parallel computation to improve independent Metropolis-Hastings based estimation. *J. Comput. Graph. Stat.* 20 (3), 616–635.
- Keeling, M.J., Eames, K.T., 2005. Networks and epidemic models. *J. R. Soc. Interface* 2 (4), 295–307.
- Keeling, M.J., Rohani, P., 2008. *Modeling Infectious Diseases in Humans and Animals*. Princeton University Press.
- Keeling, M.J., Datta, S., Franklin, D.N., Flatman, I., Wattam, A., Brown, M., Budge, G.E., 2017. Efficient use of sentinel sites: detection of invasive honeybee pests and diseases in the UK. *J. R. Soc. Interface* 14 (129).
- Lau, M.S., Gibson, G.J., Adrakey, H., McClelland, A., Riley, S., Zelner, J., Streftaris, G., Funk, S., Metcalf, J., Dalziel, B.D., et al., 2017. A mechanistic spatio-temporal framework for modelling individual-to-individual transmission-With an application to the 2014–2015 west africa ebola outbreak. *PLoS Comput. Biol.* 13 (10), e1005798.
- Liu, Q.-H., Ajelli, M., Aleta, A., Merler, S., Moreno, Y., Vespignani, A., 2018. Measurability of the epidemic reproduction number in data-driven contact networks. *Proc. Natl. Acad. Sci. USA* 115 (50), 12680–12685.
- Marjoram, P., Molitor, J., Plagnol, V., Tavaré, S., 2003. Markov chain Monte Carlo without likelihoods. *Proc. Natl. Acad. Sci. USA* 100 (26), 15324–15328.
- McKinley, T.J., Vernon, I., Andrianakis, I., McCreesh, N., Oakley, J.E., Nsubuga, R.N., Goldstein, M., White, R.G., 2018. Approximate Bayesian Computation and simulation-based inference for complex stochastic epidemic models. *Stat. Sci.* 33 (1), 4–18.
- Merler, S., Ajelli, M., Pugliese, A., Ferguson, N.M., 2011. Determinants of the spatio-temporal dynamics of the 2009 H1N1 pandemic in Europe: implications for real-time modelling. *PLoS Comput. Biol.* 7 (9), e1002205.
- Merler, S., Ajelli, M., Fumanelli, L., Gomes, M.F., Piontti, A.P., Rossi, L., Chao, D.L., Longini Jr., I.M., Halloran, M.E., Vespignani, A., 2015. Spatiotemporal spread of the 2014 outbreak of Ebola virus disease in Liberia and the effectiveness of non-pharmaceutical interventions: a computational modelling analysis. *Lancet Infect. Dis.* 15 (2), 204–211.
- Metropolis, N., Rosenbluth, A.W., Rosenbluth, M.N., Teller, A.H., Teller, E., 1953. Equation of state calculations by fast computing machines. *J. Chem. Phys.* 21 (6), 1087–1092.
- Nöremark, M., et al., 2011. Network analysis of cattle and pig movements in Sweden: measures relevant for disease control and risk based surveillance. *Prev. Vet. Med.* 99 (2), 78–90.
- Obadia, T., Silhol, R., Opatowski, L., Temime, L., Legrand, J., Thiébaud, A.C., Herrmann, J.-L., Fleury, E., Guillemot, D., Boelle, P.-Y., et al., 2015. Detailed contact data and the dissemination of *Staphylococcus aureus* in hospitals. *PLOS Comput. Biol.* 11 (3), e1004170.
- Papamakarios, G., Murray, I., 2016. Fast ϵ -free inference of simulation models with Bayesian conditional density estimation. *Adv. Neural Inf. Proc. Syst.* 1028–1036.
- Parry, S., Palmer, S., 2000. The public health significance of VTEC O157. *J. Appl. Microbiol.* 88 (S1), 1S–9S.
- Peak, C.M., Childs, L.M., Grad, Y.H., Buckee, C.O., 2017. Comparing nonpharmaceutical interventions for containing emerging epidemics. *Proc. Natl. Acad. Sci. USA* 114 (15), 4023–4028.
- Salathé, M., Kazandjieva, M., Lee, J.W., Levis, P., Feldman, M.W., Jones, J.H., 2010. A high-resolution human contact network for infectious disease transmission. *Proc. Natl. Acad. Sci. USA* 107 (51), 22020–22025.
- Schärfer, S., Widgren, S., Schwermer, H., Lindberg, A., Vidondo, B., Zinsstag, J., Reist, M., 2015. Evaluation of farm-level parameters derived from animal movements for use in risk-based surveillance programmes of cattle in Switzerland. *BMC Vet. Res.* 11 (1), 149.
- Sisson, S.A., Fan, Y., Beaumont, M., 2018. *Handbook of Approximate Bayesian Computation*. Chapman and Hall/CRC.
- Stehlé, J., Voirin, N., Barrat, A., Cattuto, C., Colizza, V., Isella, L., Régis, C., Pinton, J.-F., Khanafer, N., Van den Broeck, W., et al., 2011. Simulation of an SEIR infectious disease model on the dynamic contact network of conference attendees. *BMC Med.* 9 (1), 87.
- Toth, D.J., Leecaster, M., Pettey, W.B., Gundlapalli, A.V., Gao, H., Rainey, J.J., Uzicanin, A., Samore, M.H., 2015. The role of heterogeneity in contact timing and duration in network models of influenza spread in schools. *J. R. Soc. Interface* 12 (108), 20150279.
- Vidic, J., Manzano, M., Chang, C.-M., Jaffrezic-Renault, N., 2017. Advanced biosensors for detection of pathogens related to livestock and poultry. *Vet. Res.* 48 (1), 11.
- Vidovic, S., Korber, D.R., 2006. Prevalence of *Escherichia coli* O157 in Saskatchewan cattle: characterization of isolates by using random amplified polymorphic DNA PCR, antibiotic resistance profiles, and pathogenicity determinants. *Appl. Environ. Microbiol.* 72 (6), 4347–4355.
- Walters, C.E., Meslé, M.M., Hall, I.M., 2018. Modelling the global spread of diseases: a review of current practice and capability. *Epidemics* 25, 1–8.
- Widgren, S., Söderlund, R., Eriksson, E., Fasth, C., Aspan, A., Emanuelson, U., Alenius, S., Lindberg, A., 2015. Longitudinal observational study over 38 months of verotoxinogenic *E. coli* O157:H7 status in 126 cattle herds. *Prev. Vet. Med.* 121 (3–4), 343–352.
- Widgren, S., Engblom, S., Bauer, P., Frössling, J., Emanuelson, U., Lindberg, A., 2016. Data-driven network modelling of disease transmission using complete population movement data: spread of VTEC O157 in Swedish cattle. *Vet. Res.* 47 (1), 81. <https://doi.org/10.1186/s13567-016-0366-5>.
- Widgren, S., Bauer, P., Eriksson, R., Engblom, S., 2019. SimInf: an R package for data-driven stochastic disease spread simulations. *J. Stat. Softw.* 91 (12), 1–42.
- Widgren, S., et al., 2018. Spatio-temporal modelling of verotoxinogenic *E. coli* O157 in cattle in Sweden: exploring options for control. *Vet. Res.* 49 (78). <https://doi.org/10.1186/s13567-018-0574-2>.
- Wood, S.N., 2010. Statistical inference for noisy nonlinear ecological dynamic systems. *Nature* 466 (7310), 1102–1104.
- Zhang, C., Zhou, S., Miller, J.C., Cox, I.J., Chain, B.M., 2015. Optimizing hybrid spreading in metapopulations. *Sci. Rep.* 5, 9924.
- Zhang, Q., Sun, K., Chinazzi, M., Piontti, A.P., Dean, N.E., Rojas, D.P., Merler, S., Mistry, D., Poletti, P., Rossi, L., et al., 2017. Spread of Zika virus in the Americas. *Proc. Natl. Acad. Sci. USA* 114 (22), E4334–E4343.